Low-temperature thermal transport measurements of oxygen-annealed $Yb_2Ti_2O_7$

W. H. Toews,[1] J. A. Reid,[1] J. D. Thompson,[2] D. Prabhakaran,[2] R. Coldea,[2] and R. W. Hill[1]
[1]*Department of Physics and Astronomy, University of Waterloo, Waterloo, Ontario, Canada N2L 3G1*
[2]*Clarendon Laboratory, University of Oxford, Parks Road, Oxford OX1 3PU, United Kingdom*

(Received 4 July 2018; revised 27 May 2020; accepted 30 June 2020; published 20 July 2020)

Low-temperature thermal conductivity measurements have been conducted on an oxygen-annealed single crystal of $Yb_2Ti_2O_7$ from 60 mK to 50 K and in magnetic fields up to 8 T applied in the [111] crystallographic direction. The temperature dependence of the conductivity in zero field shows a significant peak in thermal conductivity at $T \sim 13$ K and a sharp anomaly at $T_c \sim 0.2$ K suggesting that the sample's behavior is representative of the high-purity limit, with low levels of disorder. The magnetic field dependence of the thermal conductivity close to T_c reveals a reentrant magnetic phase for a field in the [111] direction. With this information, analysis of the very low magnetic field behavior of the thermal conductivity suggests the presence of significant fluctuations close to the phase line.

DOI: 10.1103/PhysRevB.102.014434

I. INTRODUCTION

The realization that there is a considerable wealth of new physics to explore beyond the standard classifications defined by theories of broken symmetry is driving much of current condensed-matter research. One example is the search for a quantum spin liquid where quantum fluctuations prevent magnetic order down to zero temperature and stabilize exotic quasiparticle excitations. While there are many theoretical models that could potentially display such physics, one in particular that is receiving much attention is the quantum spin-ice model because it appears likely that it could apply to real material systems. The materials under consideration are the frustrated magnetic pyrochlores.

The quantum spin-ice (QSI) Hamiltonian has been shown theoretically to support a quantum spin-liquid (QSL) state at low temperature for a certain range of exchange parameters [1,2]. It differs from its classical spin-ice counterpart through the introduction of transverse magnetic coupling terms in addition to the Ising terms that exist in the classical version. The transverse terms provide the mechanism for quantum mechanical fluctuations necessary for the spin-liquid phase. When cast in a field-theoretical framework, there are three emergent excitations of the QSI on differing energy scales [2]. At the lowest-energy scale are gapless and linearly dispersing photon modes. At the highest-energy scale, given by the magnitude of the Ising interaction, are quantum monopole excitations created by spin flips. These distinguish themselves from the monopoles in classical spin-ice models by virtue of the fact that they are dispersing. On an intermediate energy scale set by the energy of the ring-exchange interaction are visons, which emerge from the termination of electric flux loops created by resonating ring-exchange plaquettes [2]. It is an experimental goal to detect these excitations in appropriate material systems.

The pyrochlore material $Yb_2Ti_2O_7$ (YbTO), with inherent magnetic frustration, has been considered as a potential candidate QSI model. Early experimental studies have been plagued by materials issues. For example, early μSR measurements showed a suppression of spin fluctuations below $T_c \sim 240$ mK [3]. However, complementary neutron scattering measurements showed no signs of magnetic order below this temperature [3–7]. On the other hand, there have also been a number of neutron scattering measurements that do exhibit ferromagnetic ordering below the critical temperature [8,9]. Additionally, a strong sample dependence is observed in the behavior of the low-temperature specific heat. Samples prepared as a powder tend to exhibit a sharp peak at temperatures up to 265 mK, whereas single crystals grown via the floating-zone technique show a broad peak at much lower temperatures, or even multiple peaks [10–12].

More recently, materials issues are starting to be resolved and control of the material stoichiometry appears to be the issue with differing or off-stoichiometry samples having different ground states [13]. It has been shown that single crystals grown via the floating-zone technique can have an excess of Yb^{3+} ions on the Ti^{4+} sublattice, known as stuffing [14]. In order to maintain charge neutrality, the oxygen stoichiometry is reduced such that the chemical formula is of the form $Yb_{2+x}Ti_{2-x}O_{7-x/2}$ [13,15]. Oxygen deficiency in these materials can affect the color and transparency of the single crystals [13,15,16]. The oxygen concentration can be controlled during the growth process by altering the composition and pressure of the growth atmosphere or by annealing the single crystals in oxygen after synthesis which reduces the disorder associated with oxygen deficiency.

With this insight into the material, it is important to now work with high-quality samples where steps have been taken to mitigate instances of nonstoichiometric growth. This will allow a consensus to emerge as to the true nature of the ground state of stoichiometric YbTO and its low temperature and magnetic field properties.

As a consequence of this approach, the following picture is starting to emerge. Stoichiometric YbTO enters a magnetically ordered ground state below a transition temperature of $T_c \sim 200$–260 mK [17–21].

The exact nature of the magnetic structure has yet to be completely established. However, the majority of studies on stoichiometric powder samples [18,22] and single crystals [20,21] suggest a spontaneous net ferromagnetic polarization along the direction of one of the cubic axes with moments canted slightly toward their local ⟨111⟩ axes. It remains an open question as to whether this canting occurs in a spin-ice-like, 2-in-2-out fashion [20,22] or in an all-in-all-out arrangement [18,21]. Neutron diffraction measurements above the critical temperature T_c reveal a rich structure of the diffuse scattering, which has been interpreted as being due to a potential proximity to a magnetic Coulomb phase [9] or originating from fluctuations due to proximity to the phase boundary between the splayed ferromagnet and other phases with antiferromagnetic order [17,23].

Thermal conductivity measurements are a reliable probe for detecting bulk quasiparticle excitations and revealing information about the spin dynamics of magnetic insulators. These measurements can also be used to detect phase transitions due to the existence of heat-carrying quasiparticles in exotic phases, or by observing variations in the level of phonon scattering from magnetic excitations. In high-quality single-crystal samples it is also possible to observe the effect of magnetic fields in different crystallographic directions. This makes thermal conductivity measurements a good choice for shedding light on the novel magnetic behavior of YbTO. Furthermore, comparison with classical spin-ice materials will provide additional information on where quantum effects are modifying the behavior.

Previous thermal transport measurements have been conducted on single crystals of YbTO [24,25]. Both studies report a quadratic temperature dependence of the thermal conductivity which is possibly due to phonon scattering from magnetic excitations. A kinklike anomaly is observed at approximately 200 mK which is related to the first-order magnetic phase transition observed in the specific heat. The field dependence of the conductivity provides evidence for a magnetic contribution to the conductivity attributed by [25] to magnetic monopole excitations for $T > 200$ mK which are suppressed with the application of a magnetic field. The low-field conductivity for $T < 200$ mK is consistent with the suppression of phonon scattering from spin fluctuations in a ferromagnetic state which is observed in magnetization measurements [26].

In this paper, we present additional thermal transport measurements on a YbTO single-crystal sample, which has been annealed in oxygen to ensure correct oxygen stoichiometry. A detailed study of the field dependence of the conductivity with the magnetic field parallel to the crystallographic [111] direction is also presented. The field is swept quasistatically with very fine field increments at temperatures near the phase transition in order to accurately observe the rapid suppression of the magnetic excitations with an applied field near T_c. Finally, the field-dependent conductivity also allows us to generate a field versus temperature phase diagram for YbTO with $B \parallel [111]$.

II. EXPERIMENTAL DETAILS

Thermal conductivity measurements were conducted on a single crystal of YbTO that was annealed in oxygen. The sample measured $2.1 \times 0.48 \times 0.35$ mm^3 with the [111] direction along the long axis of the sample. The conductivity was measured using the standard 1-heater-2-thermometer method [27] from $T = 60$ mK to 50 K across two cryostats. The field dependence of the conductivity was measured in fields up to 8 T and temperatures up to 1 K with both the heat current and applied field in the [111] direction. The magnetic field data have been corrected for demagnetization effects. The quasistatic sweep rate was 50 mT/min with a settling time between points of up to 1 h to ensure complete thermal equilibration after sweeping. The sample thermometers used to measure the thermal gradient were calibrated *in situ* to account for variations in the calibration between runs, and to accurately obtain the magnetoresistive correction for the resistive thermometers in field. The magnet was zeroed before every field sweep to minimize remnant fields in the superconducting magnet, which can be on the order of a few milliTesla. This is done by ramping the field positive and then negative with a decreasing magnitude of each sweep until the field reaches 0 T.

The annealed sample was obtained by initially preparing a polycrystalline sample using >99.99% pure Yb_2O_3 and TiO_2 via the standard solid-state reaction technique. The resulting powder was sintered at temperature between 1200 °C and 1300 °C for 48 h with intermittent regrinding to ensure a well-mixed sinter. The sinter was then compressed into a 10-mm-diameter rod approximately 140 mm long and sintered at 1250 °C for 6 h. Single crystals were grown in a four-mirror optical floating-zone furnace (Crystal System Inc.) in an argon environment with a growth rate of 1–2 mm/h. The as-grown crystals were oxygen deficient and hence are dark in color. The oxygen stoichiometry was improved by annealing the as-grown sample at 1200 °C for 72 h in a flowing oxygen atmosphere. This caused the single crystal to become transparent, a sign of stoichiometric oxygen content.

III. RESULTS

A. Zero-field temperature dependence

We will start by exploring how the thermal conductivity of YbTO is modified by annealing in oxygen and what this can reveal in terms of the level of disorder in the sample. The upper panel of Fig. 1 shows the thermal conductivity between 0.06 and 50 K for our annealed YbTO sample. As a comparison, the thermal conductivity measured by Li *et al.* [24] is also plotted. Each sample shows a peak in the magnitude of the thermal conductivity at $T \sim 13$ K. In insulating materials, as the temperature is increased, a peak in the phonon thermal conductivity results from the competition between scattering effects in the limits of low and high temperatures. At low temperatures there is a rapid (T^3) increase in the thermal conductivity when the phonon mean-free path is limited only by the boundaries of the sample. This effect is suppressed at high temperatures when sufficient phonon modes are activated that phonon-phonon (umklapp) scattering is dominant. In-between these two limits, the lattice conductivity is limited by disorder which determines the magnitude of the resulting peak [28]. Based on these qualitative arguments, the annealed sample, which has the largest peak ($\kappa \sim 80$ mW cm^{-1} K^{-1}),

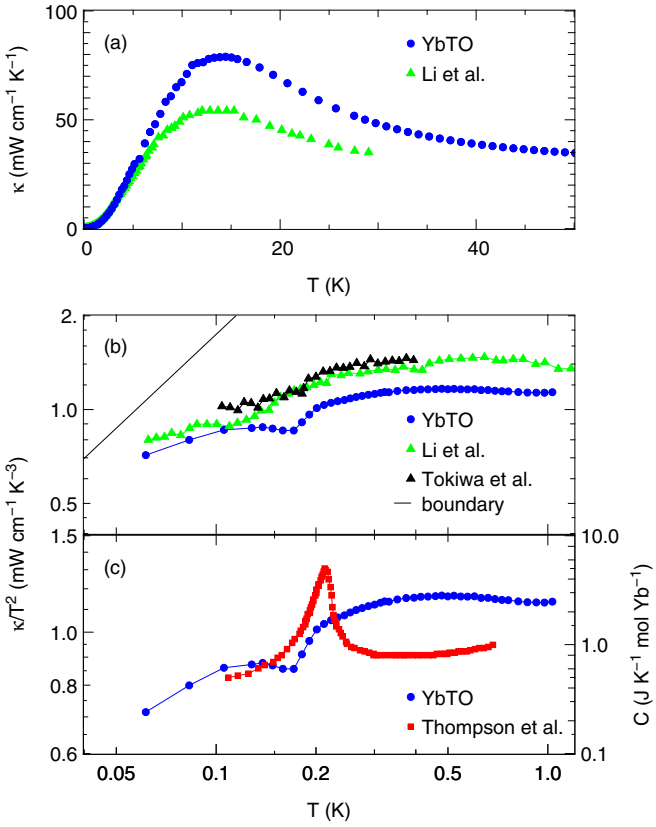

FIG. 1. (a) High-T thermal conductivity for the YbTO sample annealed in an oxygen environment (blue circles). Similar high-T conductivity on an unannealed sample by Li *et al.* [24] (green triangles). (b) Low-temperature thermal conductivity plotted as κ/T^2 versus T clearly shows a sharp anomaly associated with a magnetic transition in the annealed sample (blue circles). Similar data on other unannealed samples from the literature are presented for comparison (black triangles [25], green triangles [24]). This also illustrates the T^2 temperature dependence in samples above 200 mK. The solid black line is the calculated phonon conductivity in the boundary limited regime (see text for details). (c) Thermal conductivity plotted as κ/T^2 versus T (left axis, blue circles) for the oxygen-annealed sample in comparison to specific-heat data on a sample from the same batch and published elsewhere [19] (right axis, red squares).

has a smaller amount of disorder than the other sample presented [24]. In comparison to the classical spin-ice material $Dy_2Ti_2O_7$ (DTO), the peak measured here is about a half that measured in a high-quality single-crystal sample [29], while the unannealed sample of YbTO [24] has a peak that is similar in magnitude to as-grown samples of DTO [29].

The middle panel of Fig. 1 shows the thermal conductivity for the annealed sample plotted as κ/T^2 as a function of temperature below $T = 1$ K. Our results are qualitatively consistent with measurements reported by Li *et al.* [24] and Tokiwa *et al.* [25], which are also plotted. Also shown is the expected boundary limited, lattice conductivity based on the dimensions of the annealed sample (black line), which increases as T^3. Above $T = 0.3$ K, the constant value of κ/T^2 indicates that all samples follow a T^2 temperature dependence. This reduction from the T^3 temperature dependence expected for boundary limited phonons indicates the presence of significant phonon scattering in YbTO at zero field. However, it does not rule out the possibility of the presence of a magnetic contribution in addition to a lattice component. This aspect will be explored more fully by considering the magnetic field dependence below.

As the temperature is lowered below $T \sim 200$ mK, the annealed sample exhibits a sharp steplike transition. This feature is more prominent than anything observed in other published work on nonannealed samples [24,25] [see Fig. 1(b)]. Also plotted in Fig. 1(c) is the specific heat measured on a sample of YbTO from the same batch and having undergone an identical oxygen-annealing process [19] as the sample studied here through thermal conductivity measurements. The consistency between the transition feature in each case strongly suggests the samples are identical in their makeup. The sharpness of the peak in the specific heat reflects the fact that below T_c, the material enters a homogeneous and coherent magnetically ordered state. Likewise, the significant step in the thermal conductivity is telling us the same thing. When combined with the large peak in the thermal conductivity at higher temperatures indicating low levels of disorder [Fig. 1(a)], these observations suggest this annealed sample is in the high-purity limit.

It is instructive to compare these results with what is known about the impact of Yb-Ti stoichiometry on the magnetic ordering in this material. Arpino *et al.* [13] have shown that in single-crystal samples with exact Yb-Ti stoichiometry, the transition to a magnetically ordered state gives rise to a sharp specific-heat transition at $T_c = 264$ mK. As the Yb-Ti concentration deviates from the stoichiometric value, two things happen: the transition to the ordered state as measured by specific heat becomes broad and T_c, to the extent that it can be defined, becomes lower. This is a different response to that observed here where oxygen annealing gives rise to a sharp specific-heat transition albeit at a lower temperature ($T_c \sim 200$ mK). We do not currently have information on the Yb stoichiometry of the sample studied here, but this comparison certainly motivates further investigation to compare the effects of Yb and O stoichiometry on the magnetic properties of YbTO.

B. Magnetic field and temperature dependence

Having established the high quality of the annealed sample in comparison to those measured in earlier papers [24,25], we now explore the impact on the thermal transport for a magnetic field applied in the [111] crystallographic direction. Similar work has been presented in the literature on samples that have not undergone oxygen annealing [24,25]. The enhanced quality of the sample measured here and sharper transition allow us to track this with higher precision than has been previously possible. In Fig. 2, the temperature dependence of the thermal conductivity at various constant fields is plotted as κ/T^2. We define the transition temperature T_c as the minimum in κ/T^2 as indicated by the arrow in each plot. In zero field, $T_c = 186$ mK. Note that this definition for T_c leads to a lower-temperature value than reported for specific heat [19], but that it is not unusual for different types of measurement (e.g., transport versus thermodynamic) to yield differing values as different properties respond differently to the same transition.

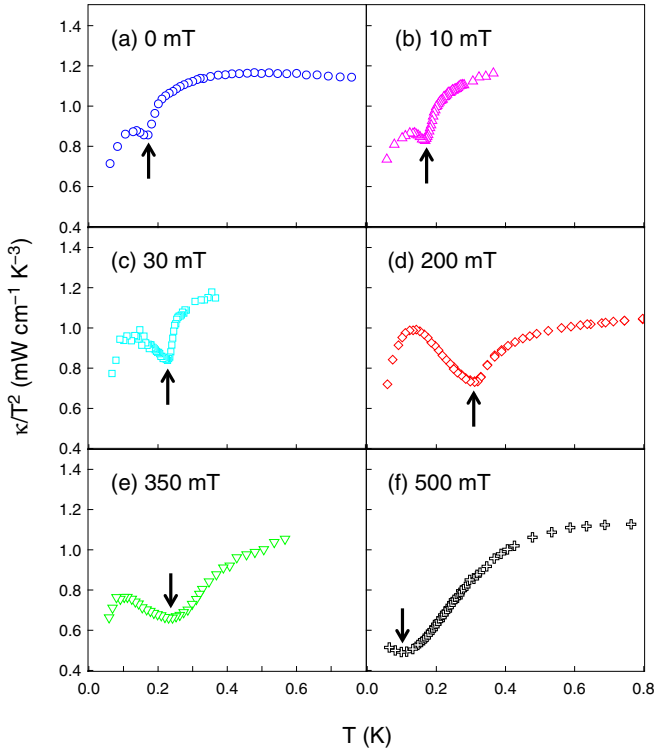

FIG. 2. The thermal conductivity of the annealed sample in applied fields up to 500 mT in the [111] direction plotted as κ/T^2 versus T. The kink in the data (indicated by the black arrows) becomes smeared out by 200 mT and is nearly fully suppressed by 500 mT.

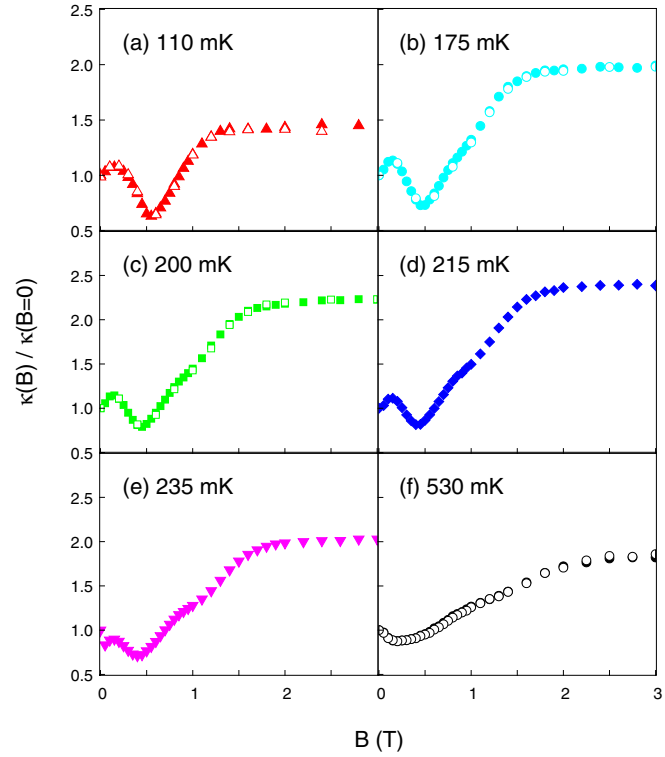

FIG. 3. The field dependence of the thermal conductivity plotted as κ/κ_o versus B at constant temperatures from 110 to 530 mK for the annealed YbTO sample. Filled (open) symbols indicate an increasing (decreasing) magnetic field.

In Fig. 3, we show the corresponding field dependence of the thermal conductivity at constant temperature. The data show the field-dependent conductivity normalized to the zero-field value $\kappa(B)/\kappa(B=0)$ for different temperatures. With the exception of the very low magnetic field behavior, the data in Figs. 2 and 3 are qualitatively consistent with that reported earlier [24,25].

The temperature and magnetic field behavior of the thermal conductivity allow us to construct a phase diagram as shown in Fig. 4. The points come from features in the data and the descriptions of the different phases come from comparison with other work, as we now explain.

C. Discussion

We now discuss the data in the context of theoretical models for quantum spin ice and earlier thermal conductivity measurements. In particular, we pay close attention to a comparison with the work that proposed an interpretation of thermal conductivity measurements in terms of quantum monopoles in YbTO [25].

In regard to models for quantum spin ice, the observation of a transition to an ordered phase at T_c suggests that stoichiometric YbTO does not have a quantum spin-liquid ground state. Nonetheless, the phase above T_c may exhibit this physics, albeit at an energy scale that precludes the likelihood of observing emergent photon excitations and visons, leaving quantum (dispersive) monopoles as the most relevant excitations for this discussion.

We start with the magnetic field and temperature dependence at temperatures above T_c as this is entirely consistent with earlier reports and has a straightforward proposal for its interpretation [24,25]. With this as our benchmark, we then approach T_c as a function of field and temperature where the results from our annealed sample allow for an improved scrutiny of the transition to the ordered phase bringing new insights to this unusual material.

At temperatures well above T_c [see Fig. 3(f)], the magnetic field dependence of the thermal conductivity has a characteristic dip at very low fields followed by gradual increase to a saturated field-independent regime. In zero field at $T \sim 0.5$ K, YbTO has been proposed as a candidate magnetic Coulomb liquid with spin-ice correlations giving rise to monopole excitations [9]. In this scenario, as the magnetic field is increased in the [111] direction, the spin-ice correlations and monopole excitations would be expected to be suppressed. With the loss of magnetic correlations, the spins exhibit paramagnetic behavior and are gradually polarized leading to a loss of spin-phonon scattering. Within this picture, the thermal conductivity would contain contributions from monopoles and phonons and the initial decrease in thermal conductivity would be attributed to the loss of monopole conduction. In principle, this loss of thermal conductivity could also be attributed to an increase in spin-phonon scattering, leading to a reduction of phonon conductivity. However, spin-phonon scattering is very unlikely to increase with an increasing magnetic field. Beyond the initial dip, and as reported earlier [25], the increase in the thermal conductivity with magnetic field in the

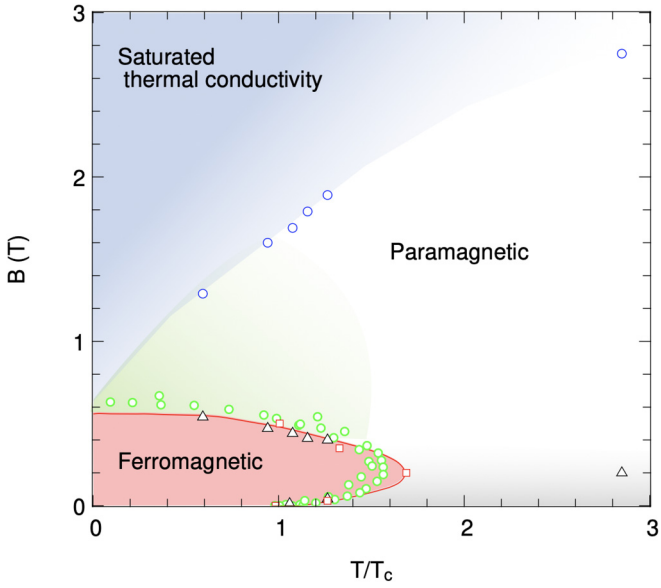

FIG. 4. Field versus temperature phase diagram for YbTO for $B \parallel [111]$ extracted from thermal conductivity measurements on our oxygen-annealed sample. The temperature axis is scaled by $T_c = 0.186$ K (0.264 K) for this work (Ref. [20]). The open blue, black, and red symbols are extracted from the temperature- and field-dependent thermal conductivity data. The phase lines are guides to the eye and crossover regions are indicated by shading. The gray shaded region indicates where the thermal conductivity shows an initial decrease with increasing magnetic field, which is consistent with a suppression of thermal conductivity carried by magnetic excitations. Green circles are from specific heat, magnetization, and neutron scattering measurements on a YbTO stoichiometric sample with $T_c = 264$ mK [20].

paramagnetic region is consistent with a reduction in scattering by paramagnetic spins. Strong evidence for this is provided by B/T scaling [25], which we also observe in our measurements (not shown). At the highest magnetic fields probed, the spins are becoming progressively polarized along the field and the thermal conductivity is observed to be field independent and entirely due to phonons scattered only by disorder.

Returning to the proposals for exotic quantum monopole excitations in YbTO, the decrease in conductivity at low fields has been proposed as evidence for monopole conductivity [24,25]. In particular, it has been proposed that the large magnitude of this decrease in comparison to classical spin-ice materials (DTO, HTO) could be evidence for a more dispersing (quantum) monopole. However, we note that the magnitude of the suppression in conductivity will depend on a variety of factors such as the magnitude of the monopole conductivity (which may depend on the level of disorder in the material [29]), and the magnitude of the spin-phonon scattering. Moreover, the magnitude of the suppression measured in YbTO, approximately 20% of the total conductivity, is not significantly different from that reported in similar measurements on classical spin-ice materials [24,29–32].

In zero magnetic field, as the temperature is lowered through T_c there is a steplike decrease in thermal conductivity. Earlier papers [24,25] have proposed that the origin of this decrease is most likely the loss of the thermal transport contribution from monopoles in the magnetic Coulomb liquid. Moreover, the magnitude of the decrease in conductivity is approximately the same as the decrease in thermal conductivity when a magnetic field is applied above T_c, which we have already discussed extensively above. The temperature dependence of the thermal conductivity below T_c can in principle provide clues as to the nature of the magnetic order that is observed using other techniques [20]. The data in Fig. 1(b) show that the temperature dependence increases its power-law behavior above T^2, which is seen in the region above T_c, but does not quite reach the T^3 behavior expected for phonons in the boundary scattering limit. Moreover, the magnitude is below that expected given the sample size [see Fig. 1(b)]. Exploring the magnetic field or temperature dependence within the low-temperature phase [see Figs. 2(a)–2(e) and 3(a)–3(e)], the thermal conductivity shows a local maximum at the center of this phase. Whether the conductivity is attributed to phonons or magnetic excitations or a combination of both cannot be conclusively determined, however, the dependence is consistent with significant magnetic fluctuations that increase as the phase boundary is approached. The observation of sizable fluctuations in this low-temperature magnetic phase is consistent with a number of other measurements [19,20,22]. To explore this further will require measurements down to lower temperatures and additional theoretical input.

Next, we discuss the unusual temperature and field dependence of the transition temperature T_c itself. It is already apparent from Figs. 2(a)–2(d) that the application of a small [111] magnetic field causes T_c to increase. Beyond a field of approximately 200 mT, the transition temperature decreases. This results in a reentrant phase at low temperatures and low magnetic fields, as shown in Fig. 4. This is entirely consistent with the phase diagram deduced for a stoichiometric Yb-Ti sample from magnetization, specific-heat, and neutron scattering experiments in a [111] magnetic field that is reported by Scheie *et al.* [20] and reproduced in Fig. 4 and also observed for a magnetic field along [110] [33]. The use of a reduced temperature axis in the phase diagram shows that, in spite of the differences in T_c between our oxygen-annealed sample ($T_c \sim 200$ mK) and an Yb-Ti stoichiometric sample ($T_c \sim 264$ mK) [20], the coherent magnetic phase that the material enters has the same reentrant magnetic phase line. Close scrutiny of measurements made with magnetic fields sweeping in opposite directions does not reveal any hysteresis (see Fig. 3), which supports the idea that the magnetic phase transitions are second order [33]. The phase diagram also denotes three other regions outside the magnetically ordered phase. In the high-field limit, we denote the region where the thermal conductivity becomes field independent (saturated thermal conductivity). This is consistent with the spins being progressively more polarized by the applied field leading to a loss of magnetic scattering of the lattice conductivity. In the low-field limit above T_c, we denote the region where the thermal conductivity initially decreases (light gray region), which we have noted could be consistent with the presence of monopole excitations and may therefore correlate with magnetic Coulomb liquid phase [9]. In-between these two limits is the paramagnetic region where we observe an increasing

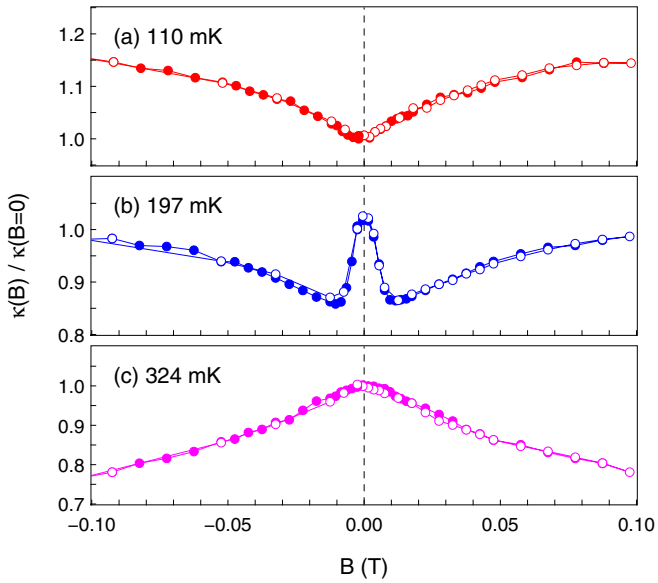

FIG. 5. The low-field thermal conductivity of the annealed sample normalized by its value in zero magnetic field, for $B < 0.1$ T measured at (a) 110 mK (red), (b) 197 mK (blue), and (c) 324 mK (magenta). To correct for residual magnetic field in the superconducting magnet, the data have been symmetrized by shifting in field by −2.0, −2.5, and −2.5 mT, respectively.

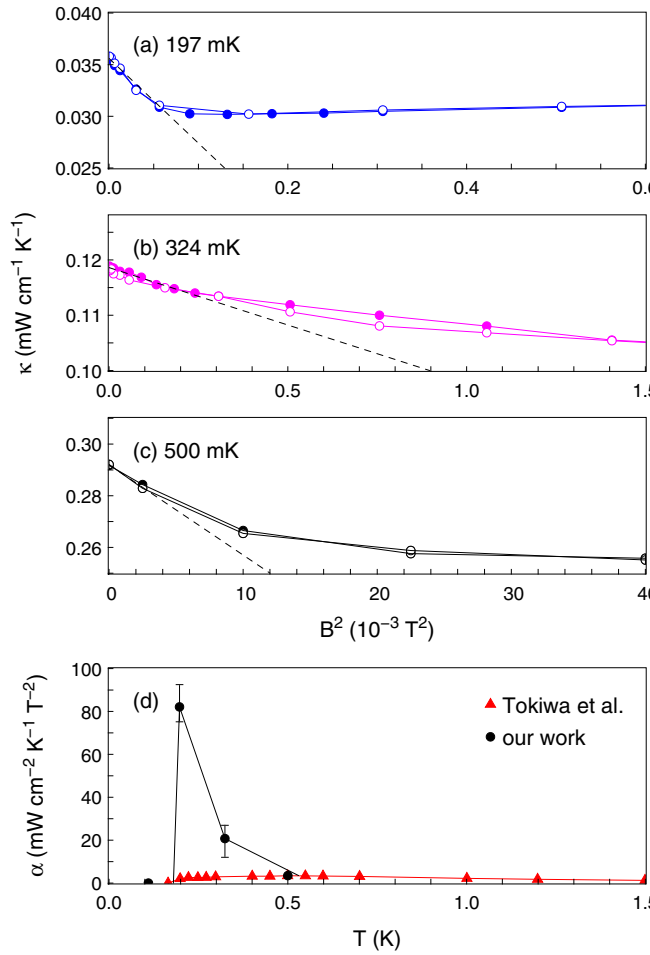

FIG. 6. The thermal conductivity plotted versus the square of the magnetic field B^2 measured at temperatures of (a) 197 mK, (b) 324 mK, and (c) 500 mK. The solid lines are linear fits to the data as $B \to 0$ T. The slope of this fit is the magnitude of α. (d) The temperature dependence of the conductivity suppression rate α (see text) extracted from measurements of the low field and temperature conductivity. The suppression rate measured by Tokiwa *et al.* [25] (red triangles) shows a peak at $T_{max} = 500$ mK. Conversely, the magnitude of α extracted from measurements on our annealed sample (black circles) increases monotonically until T_c.

thermal conductivity with magnetic field with B/T scaling and consistent with spin-phonon scattering.

This reentrant nature of the phase diagram suggests a reexamination of the "quantum monopole" picture based on earlier thermal conductivity measurements in a [111] magnetic field by Tokiwa *et al.* [25]. As in that paper, we track the rate at which the thermal conductivity is suppressed when a magnetic field is first applied as a function of temperature close to T_c, where YbTO will enter the ferromagnetic phase before the paramagnetic phase ($T \lesssim 320$ mK). Our results are shown in Figs. 5 and 6.

In Fig. 5, the magnetic field dependence of the thermal conductivity normalized by its value in zero field is shown at three representative temperatures. The magnetic field is swept through zero, about which point the data are symmetrized by shifting the magnetic field axis by a constant amount (on the order of a few milliTesla). This accounts for any residual magnetic field in the superconducting magnet. In Fig. 5(a), $T = 110$ mK, the data are measured below T_c, where there is no initial decrease with increasing magnetic field consistent with the absence of magnetic excitations that exist above T_c. In Fig. 5(b), $T = 197$ mK, the data are measured just above T_c. In Fig. 5(c), $T = 324$ mK, the temperature is close to the maximum of the reentrant ferromagnetic phase. For both temperatures above T_c [Figs. 5(b) and 5(c)], the field dependence of the thermal conductivity shows an initial decrease with increasing magnetic field. This has been proposed to show how quickly the monopole conductivity is suppressed by a magnetic field as the temperature is lowered toward T_c [25].

Following [25], in Figs. 6(a)–6(c), we parametrize the magnitude of the suppression rate with field by α, according to $\kappa(B) = \kappa(0) - \alpha B^2$. This is shown by the dotted line in each panel, which is a fit to the data as B^2 approaches zero. The slope of each fit is the magnitude of α. The temperature dependence of $\alpha(T)$ from this work is shown in Fig. 6(c) (black) in comparison to the results from [25] (red). The results are clearly different; where our work shows that $\alpha(T)$ effectively diverges as T_c is approached, Tokiwa *et al.* report a nonmonotonic temperature dependence. The difference in these results may be technical or may be related to sample dependence in YbTO [13]. On the technical side, the field scale for the suppression at $T = 197$ mK is 10 mT, which is on the order of the remnant field in most superconducting magnets. Only by sweeping the magnetic field through zero and measuring at both positive and negative magnetic fields can the field zero be accurately determined, as seen in Fig. 5(b). Alternatively, increased disorder or a difference in stoichiometry of the YbTO sample being measured may result in different magnetic ground-state order [21]. In any

case, the clear monotonic behavior of α in this work does not support the idea of a reduced monopole gap associated with a dispersive quantum monopole, as proposed earlier [25].

The origin of the suppression of the thermal conductivity with magnetic field and therefore the divergence of α is complicated by the proximity of the first-order transition to the ordered ferromagnetic phase. The temperature and field dependence of the thermal conductivity will be a combination of a potential change in heat carrier in moving from one phase to the other along with a change in scattering of the heat-carrying excitations. These effects will be difficult to disentangle without further theoretical insight.

Nonetheless, we can make a couple of statements about these experimental observations. First, there is the possibility of ferromagnetic fluctuations which can influence the thermal conductivity through the scattering of heat carriers. However, the phase transition in pristine samples exhibits hysteresis [20], which points to a first-order transition and therefore the absence of critical fluctuations near T_c, as expected for a second-order transition. Note that the hysteresis causes a shift in the transition temperature at the level of a few milliKelvin, which is beyond the resolution of our thermal conductivity measurements.

Next, we consider the effect of putative quantum fluctuations, which we have already discussed in the context of the suppressed transition temperature in zero magnetic field. While it would be insightful to establish the influence of quantum fluctuation through a comparison with the thermal conductivity behavior of a classical spin-ice system such as $Dy_2Ti_2O_7$ or $Ho_2Ti_2O_7$, this is simply unrealistic because of the influence of disorder on the magnitude and temperature dependence of monopole conductivity [29]. What can be said is that an increased suppression rate of thermal conductivity as the temperature is lowered toward T_c is certainly consistent with the presence of an additional scattering mechanism for the magnetic (and phonon) conductivity, which may point to the presence of significant quantum fluctuations.

IV. SUMMARY AND CONCLUSION

Temperature- and field-dependent thermal transport measurements have been conducted on a YbTO sample, which has been annealed in oxygen. Our results reveal that, in comparison to samples reported in previous thermal conductivity studies [24,25], the annealed sample has a lower level of defect scattering of phonons and also shows a sharp, steplike feature at the magnetic transition temperature $T_c \sim 200$ mK. The [111] magnetic field-dependent study has shown that magnetic monopole excitations contribute a significant amount to the total thermal transport when $T > T_c$ which is consistent with previously reported thermal conductivity data [24,25]. Consequently, although variances in the oxygen stoichiometry affect the phonon channel of conductivity and the behavior of the low-temperature transition, it appears that they do not play a significant role in the behavior of the magnetic excitations in YbTO above T_c. Furthermore, contrary to the work of Tokiwa *et al.* [25], we find that in our annealed sample, the suppression rate of the magnetic excitations with magnetic field exhibits a monotonic increase as $T \to T_c^+$, in contrast to earlier reports of a nonmonotonic temperature dependence in unannealed samples [25]. This suggests that oxygen order may affect the low-temperature low-field behavior of magnetic excitations in this material [21].

The [111] magnetic field versus temperature phase diagram extracted from our conductivity data reveals a reentrant ferromagnetic phase below ~200 mK and 600 mT. This is consistent with recent magnetization, specific-heat, and neutron scattering measurements on samples in which the Yb-Ti ratio is stoichiometric, where $T_c = 264$ mK [20,21]. This observation suggests that while the Yb-Ti stoichiometry might not be tightly controlled in our oxygen-annealed samples, this does not have a qualitative impact on the magnetic properties in spite of a reduction of T_c. The interplay between oxygen stoichiometry and order and Yb-Ti stoichiometry remains an outstanding question in this unique material.

ACKNOWLEDGMENTS

This research was supported by NSERC of Canada. Work in Oxford was partially supported by EPSRC (UK) through Grants No. EP/H014934/1 and No. EP/K028960/1. J.D.T. acknowledges support from the University of Oxford Clarendon Fund and NSERC of Canada. R.W.H. would like to thank the Cavendish Laboratory and Corpus Christi College, University of Cambridge, for their kind hospitality during the final preparation of this manuscript.

[1] L. Savary and L. Balents, Phys. Rev. Lett. **108**, 037202 (2012).

[2] M. J. P. Gingras and P. A. McClarty, Rep. Prog. Phys. **77**, 056501 (2014).

[3] J. A. Hodges, P. Bonville, A. Forget, A. Yaouanc, P. Dalmas de Réotier, G. André, M. Rams, K. Królas, C. Ritter, P. C. M. Gubbens, C. T. Kaiser, P. J. C. King, and C. Baines, Phys. Rev. Lett. **88**, 077204 (2002).

[4] J. S. Gardner, G. Ehlers, N. Rosov, R. W. Erwin, and C. Petrovic, Phys. Rev. B **70**, 180404(R) (2004).

[5] P. Bonville, J. A. Hodges, E. Bertin, J.-P. Bouchaud, P. D. de Réotier, L.-P. Regnault, H. M. Rønnow, J.-P. Sanchez, S. Sosin, and A. Yaouanc, Transitions and spin dynamics at very low temperature in the pyrochlores $Yb_2Ti_2O_7$ and $Gd_2Sn_2O_7$, in *ICAME 2003: Proceedings of the 27th International Conference on the Applications of the Mössbauer Effect (ICAME 2003) held in Muscat, Oman, 21–25 September 2003*, edited by M. E. Elzain, A. A. Yousif, A. D. al Rawas, and A. M. Gismelseed (Springer, Dordrecht, 2004), pp. 103–111.

[6] K. A. Ross, J. P. C. Ruff, C. P. Adams, J. S. Gardner, H. A. Dabkowska, Y. Qiu, J. R. D. Copley, and B. D. Gaulin, Phys. Rev. Lett. **103**, 227202 (2009).

[7] K. A. Ross, L. R. Yaraskavitch, M. Laver, J. S. Gardner, J. A. Quilliam, S. Meng, J. B. Kycia, D. K. Singh, T. Proffen, H. A. Dabkowska, and B. D. Gaulin, Phys. Rev. B **84**, 174442 (2011).

[8] Y. Yasui, M. Soda, S. Iikubo, M. Ito, M. Sato, N. Hamaguchi, T. Matsushita, N. Wada, T. Takeuchi, N. Aso, and K. Kakurai, J. Phys. Soc. Jpn. **72**, 3014 (2003).

[9] L.-J. Chang, S. Onoda, Y. Su, Y.-J. Kao, K.-D. Tsuei, Y. Yasui, K. Kakurai, and M. R. Lees, Nat. Commun. **3**, 992 (2012).
[10] A. Yaouanc, P. Dalmas de Réotier, C. Marin, and V. Glazkov, Phys. Rev. B **84**, 172408 (2011).
[11] K. A. Ross, L. Savary, B. D. Gaulin, and L. Balents, Phys. Rev. X **1**, 021002 (2011).
[12] R. M. D'Ortenzio, H. A. Dabkowska, S. R. Dunsiger, B. D. Gaulin, M. J. P. Gingras, T. Goko, J. B. Kycia, L. Liu, T. Medina, T. J. Munsie, D. Pomaranski, K. A. Ross, Y. J. Uemura, T. J. Williams, and G. M. Luke, Phys. Rev. B **88**, 134428 (2013).
[13] K. E. Arpino, B. A. Trump, A. O. Scheie, T. M. McQueen, and S. M. Koohpayeh, Phys. Rev. B **95**, 094407 (2017).
[14] K. A. Ross, T. Proffen, H. A. Dabkowska, J. A. Quilliam, L. R. Yaraskavitch, J. B. Kycia, and B. D. Gaulin, Phys. Rev. B **86**, 174424 (2012).
[15] D. Prabhakaran and A. Boothroyd, J. Cryst. Growth **318**, 1053 (2011).
[16] G. Balakrishnan, O. A. Petrenko, M. R. Lees, and D. M. Paul, J. Phys.: Condens. Matter **10**, L723 (1998).
[17] J. Robert, E. Lhotel, G. Remenyi, S. Sahling, I. Mirebeau, C. Decorse, B. Canals, and S. Petit, Phys. Rev. B **92**, 064425 (2015).
[18] A. Yaouanc, P. Dalmas de Réotier, L. Keller, B. Roessli, and A. Forget, J. Phys.: Condens. Matter **28**, 426002 (2016).
[19] J. D. Thompson, P. A. McClarty, D. Prabhakaran, I. Cabrera, T. Guidi, and R. Coldea, Phys. Rev. Lett. **119**, 057203 (2017).
[20] A. Scheie, J. Kindervater, S. Säubert, C. Duvinage, C. Pfleiderer, H. J. Changlani, S. Zhang, L. Harriger, K. Arpino, S. M. Koohpayeh, O. Tchernyshyov, and C. Broholm, Phys. Rev. Lett. **119**, 127201 (2017).
[21] D. Bowman, E. Cemal, T. Lehner, A. Wildes, L. Mangin-Thro, G. Nilsen, M. Gutman, D. Voneshen, D. Prabhakaran, A. Boothroyd, D. G. Porter, C. Castelnovo, K. Refson, and J. Goff, Nat. Commun. **10**, 637 (2019).
[22] J. Gaudet, K. A. Ross, E. Kermarrec, N. P. Butch, G. Ehlers, H. A. Dabkowska, and B. D. Gaulin, Phys. Rev. B **93**, 064406 (2016).
[23] L. D. C. Jaubert, O. Benton, J. G. Rau, J. Oitmaa, R. R. P. Singh, N. Shannon, and M. J. P. Gingras, Phys. Rev. Lett. **115**, 267208 (2015).
[24] S. J. Li, Z. Y. Zhao, C. Fan, B. Tong, F. B. Zhang, J. Shi, J. C. Wu, X. G. Liu, H. D. Zhou, X. Zhao, and X. F. Sun, Phys. Rev. B **92**, 094408 (2015).
[25] Y. Tokiwa, T. Yamashita, M. Udagawa, S. Kittaka, T. Sakakibara, D. Terazawa, Y. Shimoyama, T. Terashima, Y. Yasui, T. Shibauchi, and Y. Matsuda, Nat. Commun. **7**, 10807 (2016).
[26] E. Lhotel, S. R. Giblin, M. R. Lees, G. Balakrishnan, L. J. Chang, and Y. Yasui, Phys. Rev. B **89**, 224419 (2014).
[27] W. H. Toews and R. W. Hill, Rev. Sci. Instrum. **85**, 043905 (2014).
[28] J. M. Ziman, *Electrons and Phonons: The Theory of Transport Phenomena in Solids*, edited by N. F. Mott, E. C. Bullard, and D. H. Wilkinson (Oxford University Press, Oxford, 1963), pp. 288–326.
[29] W. H. Toews, J. A. Reid, R. B. Nadas, A. Rahemtulla, S. Kycia, T. J. S. Munsie, H. A. Dabkowska, B. D. Gaulin, and R. W. Hill, Phys. Rev. B **98**, 134446 (2018).
[30] G. Kolland, M. Valldor, M. Hiertz, J. Frielingsdorf, and T. Lorenz, Phys. Rev. B **88**, 054406 (2013).
[31] C. Fan, Z. Y. Zhao, H. D. Zhou, X. M. Wang, Q. J. Li, F. B. Zhang, X. Zhao, and X. F. Sun, Phys. Rev. B **87**, 144404 (2013).
[32] S. Scharffe, G. Kolland, M. Hiertz, M. Valldor, and T. Lorenz, JPS Conf. Proc. **3**, 014030 (2014).
[33] S. Säubert, A. Scheie, C. Duvinage, J. Kindervater, S. Zhang, H. J. Changlani, G. Xu, S. M. Koohpayeh, O. Tchernyshyov, C. L. Broholm, and C. Pfleiderer, Phys. Rev. B **101**, 174434 (2020).